Thermal stability of mesoporous silica-coated gold nanorods with different aspect ratios

Eszter Gergely-Fülöp[a], Dániel Zámbó[b] and András Deák[c]

Institute for Technical Physics and Materials Science, HAS Research Centre for Natural Sciences, P.O. Box 49., H-1525 Budapest, Hungary

[a]E-mail: fulop.eszter@ttk.mta.hu
[b]E-mail: zambo.daniel@ttk.mta.hu
[c]Corresponding author, E-mail: deak.andras@ttk.mta.hu, Tel: +36 1 392 2602, Fax: +36 1 392 2226

Abstract

The effect of different temperatures (up to 900 °C) on the morphology of mesoporous silica-coated gold nanorods was systematically investigated. Gold nanorods with different aspect ratios (AR ranging from 2.5 to 4.3) were coated with a 15 nm thick mesoporous silica shell. Silicon supported monolayers of the particles were annealed in the temperature range of 300-900 °C. The resulting changes in particle morphology were investigated using scanning electron microscopy and visible wavelength extinction spectroscopy. The silica coating generally improved the stability of the nanorods from ca. 250 °C by several hundreds degree Celsius. For nanorods with AR<3 the shape and the aspect ratio change is only moderate up to 700 °C. At 900 °C these nanorods became spherical. For nanorods with AR>3, lower stability was found as the aspect ratio decrease was more significant and they transformed into spherical particles already at 700 °C. It was confirmed by investigating empty silica shells that the observed conformal change of the shell material when annealing core/shell particles is dictated by the deformation of the core particle. This also implies that a significant mechanical stress is exerted on the shell upon core deformation. In accordance with this, for the highest aspect ratio (AR~4) nanorod the shell breaks up at 900 °C and the gold cores were partially released and coalesced into large spherical particles.

Keywords: optical materials, annealing, deformation, optical properties

1. Introduction

Due to the special optical properties of noble metal nanoparticles, they have been studied very intensively in the last decades. The plasmonic properties of gold nanorods allow them to be used in photothermal therapy [1,2], imaging techniques [3,4], theranostics [5,6], sensing applications [7-10] and optical memories [11,12].

The shape deformation and melting point decrease of nanoparticles was observed and described earlier for different types of nanoparticles [13-16]. The lower melting point compared to the bulk material is due to the large surface-to-volume ratio, which results in an increase in the surface free energy of the particles [17]. Several calculations were made to determine the melting point of nanoparticles with different size and shape [13,14,18-20]. For bulk gold the melting point is at 1064 °C [21], whereas for gold nanoparticles it can be found below this value. For non-spherical nanoparticles, a shape transformation into nanospheres

can be observed as the nanoparticle reduces its surface energy due to the applied heat. The melting of both spherical and rod-shaped gold nanoparticles can be interpreted in terms of surface melting [22-25], whereby there is a small difference in the melting temperatures for the different facets [26-28]. For gold nanorods the surface melting is accompanied by the transformation into nanospheres, which is explained by Insawa et al. in Ref. [23] on the basis of surface tension considerations. The decrease of the aspect ratio depends on the thickness of the liquid layer, which depends on the temperature.

The effect of high temperatures on bare (without inorganic shell) gold nanorods was investigated experimentally by optical heating *via* laser pulses [29-33] or annealing solid supported gold nanorods [34,35] using bulk-heating. Hu et al. investigated the heating of the nanorods between 180 °C and 500 °C using bulk-annealing [34]. They found that at 180 °C the nanorods coalesce into irregular shaped clusters and at 500 °C they coalesce into large spherical particles. Petrova et al. investigated the differences between the bulk- and ultrafast laser-induced heating of nanorods [35]. For bulk-heating they found that at 250 °C the solid-supported nanorods were converted into spheres. When laser-induced heating was performed in solution, the nanorods maintained their integrity up to 700 °C. It was suggested that the higher thermal stability of the nanorods heated by short laser pulses is a result of the quick release of heat into the surrounding liquid, i.e. the nanorods are not heated long enough to allow any significant structural change.

Several methods were published about protecting gold nanorods from the heat-induced shape deformation, which is crucial in some applications, e.g. in photothermal therapy [1,2] and photoacoustic imaging [36-38]. It was shown that embedding the nanorods into a titanium-oxide matrix [39], or coating with carbon [40] or other materials [7,25] can protect them from shape transformations during heating up to ~690 °C. For silica shells, however, the temperature related shape change of the core/shell nanoparticles upon bulk heating was investigated only up to 260 °C and for aspect ratios higher than 4 [41,42]. There are several methods to create a thin silica shell on gold nanorods (e.g. Refs. [43-45]) and it has been shown that the silica coating can increase the stability of the core particles when applying bulk heating up to 260 °C [41,42]. Gautier et al. [41] interpreted this shape-protecting effect of the shell on the basis of the higher melting point of silica compared to bulk gold. This allows the silica shell to sustain its shape and protect the core particles from coalescence hence acting as a mold for the core particles to preserve their rod shape. Nevertheless, there are no systematic studies available on the bulk heating of core/shell nanorods with different

aspect ratio at high temperatures. In our study we use mesoporous silica coated gold nanorods with AR ranging from 2.5 to 4.3. Based on our previous results [46] some degree of elasticity of the mesoporous shell is expected, but the question remains how the deformation of the core particle is influenced by the silica shell for different aspect ratios and how far the silica shell can sustain its integrity upon the shape change of the core particle?

In this work we investigate systematically how a mesoporous silica shell increases the stability of the gold core at high temperatures up to 900 °C. Gold nanorods with different aspect ratios were prepared and coated with a ca. 15 nm thick mesoporous silica shell. The particles were deposited onto solid substrates and these solid-supported nanoparticles were subjected to thermal treatment in an oven at different temperatures up to 900 °C. To investigate the changes in particle morphology and the plasmonic properties after annealing, scanning electron microscopy (SEM) and visible extinction spectroscopic measurements were carried out. Our results indicate that the silica coating effectively improves the thermal stability of the particles for all investigated aspect ratios. The larger aspect ratio nanorods however are more susceptible to deformation in agreement with surface energy considerations. It is confirmed that the conformal deformation of the silica shell upon annealing is dictated by the shape change of the core. For large aspect ratio nanorods, the mechanical stress during the deformation of the core results in the destruction of the silica shell.

2. Experimental section

2.1 Materials

Sodium borohydride, ReagentPlus® 99 % ($NaBH_4$); tetrachloroauric (III) acid trihydrate, ACS reagent ($HAuCl_4 \cdot 3H_2O$); cetyltrimethyl ammonium bromide, SigmaUltra 99 % (CTAB); 5-bromosalycilic acid, technical grade, 90 % (5-BSA), tetraethyl ortosilicate, puriss, 99 % (TEOS); L-ascorbic acid, ACS reagent 99 % (AA); silver nitrate, 99.9999 % metal basis ($AgNO_3$) and methanol, puriss. p.a., ACS reagent, reag. ISO, reag. Ph. Eur., ≥99.8% (MeOH) were purchased from Sigma-Aldrich. Sodium hydroxide, a.r. (NaOH) from Reanal and chloroform, reagent grade, ACS, ISO, stabilized with ethanol from Scharlau were used. All chemicals were used as received. For all experiments Milli-Q water (18.2 MOhm/cm) was used.

2.2 Synthesis of mesoporous silica-coated gold nanorods

Au1, Au2 and Au3 gold nanorods with different aspect ratios were prepared by the seeded growth method similar to Ref. [43]. The aspect ratio of the nanoparticles was varied through the contents of the growth solution.

The seed solution was prepared by mixing 2.5 ml 0.001 M $HAuCl_4$, 2.5 ml H_2O and 5 ml 0.2 M CTAB. Then, 600 µl 0.01 M ice-cold $NaBH_4$ was injected. The resulting brownish solution was vigorously stirred for ~15 s, and then stirred at 45 °C for 15 minutes.

The Au1 nanorods (AR=2.5) were synthesized by adding 40 µl seed solution to the growth solution containing 17 ml 0.0001 M $HAuCl_4$, 25 ml 0.2 M CTAB, 200 µl 0.04 M $AgNO_3$ and 238 µl 0.1 M AA.

The Au2 (AR=3.0) and the Au3 nanorods (AR=3.4) were prepared in a growth solution containing 50 ml 0.2M CTAB, 100 µl 0.04 M $AgNO_3$, 50 ml 0.001 M $HAuCl_4$ and 700 µl AA. To 20 ml of this solution, in the case of Au2 rods 200 µl, in the case of Au3 rods 600 µl seed solution was added.

In the case of Au4 nanorods, with AR=4.3 a different seeded growth method was used, according to Ref. [47]. The seed solution was made by mixing 0.5 ml 0.001 M $HAuCl_4$, 0.5 ml H_2O and 1 ml 0.2 M CTAB. Then, 0.12 ml 0.01 M ice-cold $NaBH_4$ was mixed with 0.08 ml water (room temperature) and added to this solution. After 2 minutes of vigorous stirring, it was left undisturbed for 30 minutes. The growth solution was prepared as follows: First, to 25 ml solution of 0.9 g CTAB and 0.11 g 5-BSA (30 °C), 0.96 ml 0.004 M $AgNO_3$ was added and stirred for 15 minutes. Then, 10 ml 0.001 M $HAuCl_4$ was put into the mixture, and stirred again for 15 minutes, followed by the addition of 0.07 ml 0.064 M AA and stirred for 30 seconds vigorously. Finally, 0.016 ml seed solution was injected.

The resulting solutions were left undisturbed overnight. The visible spectra of the nanoparticles were measured by using an Agilent 8453 spectrophotometer.

The silica coating procedure was carried out as reported in Ref. [48] with some modifications. First, 15 ml gold nanorod solution was centrifuged at 9500 rpm for 45 minutes at 28 °C and redispersed with 10 ml water. In the case of the Au4 nanorods, the dispersant CTAB – 5-BSA solution was changed with a 0.1 M CTAB solution by a prior centrifugation. The resulting

solution's pH was set to ~10-11 with 0.1 M NaOH. Then, 3x15 µl 20:80 TEOS:MeOH mixture was added in 30 minute intervals. This solution was stirred for 2 days, then centrifuged 5 times and redispersed in MeOH.

2.3 Preparation of monolayers on solid supports

The nanoparticle monolayers were first created at the water/air interface using a procedure reported by us earlier [48]. A methanolic solution of the nanoparticles was mixed with chloroform (in 1:2 ratio) and then spread at the air/water interface in a PTFE beaker. After the chloroform evaporated, a part of the resulting interfacial monolayer was lifted out with a silicon substrate that was cleaned prior to deposition by extensively rinsing with water, acetone and finally with water. The solid supported monolayers of the core/shell nanorods were allowed to dry under ambient conditions.

2.4 Annealing procedure

The prepared monolayers were put into an oven (MTI Corporation, GSL 1100X) and heated at different temperatures of 300, 500, 700 and 900 °C for 1 hour. The morphology of the nanoparticles was investigated by using a LEO 1540 XB field emission scanning electron microscope (5 kV acceleration voltage). The size and aspect ratio of the nanorods was calculated by averaging over 100 particles in each case. Extinction measurements were carried out using an Avantes AvaSpec-2048 fiber coupled spectrometer.

3. Results and discussion

Figure 1 shows the normalized extinction spectra of the as-prepared nanorods in solution. For each spectrum, two main extinction peaks can be observed, the transversal plasmon resonance mode at ~520 nm and the longitudinal mode at higher wavelengths. The increasing aspect ratio results in longitudinal plasmon peaks at longer wavelengths (see also Table 1), which is in agreement with earlier findings [49]. The nanorods were covered with a ca. 15 nm thick mesoporous silica shell.

The nanoparticles were deposited onto solid Si substrates then were subjected to heat treatment in an oven up to 900 °C. The size and the calculated aspect ratio of the nanorods

before and after the heat treatment and the corresponding longitudinal peak positions are listed in Table 1. The resulting spectral and structural changes upon heating for each sample are presented in the Supporting Information (Figure S1-S4). For better overview the longitudinal peak position and the aspect ratio of the samples are plotted as a function of temperature in Figure 2. As an example the extinction spectra of the Au1 particles before and after heat treatments are shown in Figure 3.

For the Au1 nanorods the AR remains almost unchanged up to 500 °C, while at 700 °C decreases significantly which causes a large blue shift in the LSPR peak position (Figure 3). At 900 °C the Au1 nanoparticles became sphere-like with AR=1.4 (see Table 1 and Figure 4.a,b).

As a result of the heat treatment at 300 °C, significant aspect ratio decrease occurred in the case of nanorods Au2-Au4 (Figure S2-4.b-c). For the Au4 particles this decrease is very steep as compared to the Au2 and Au3 ones (see Figure 2). This shape change simultaneously causes the blue shift of the longitudinal peak position. The gold cores' AR changed monotonously in the case of Au2 and Au3 particles and they turned into nanospheres at 900 °C.

Nanoparticles with AR>3 show less stability compared to nanoparticles with AR≤3, since the gold cores became sphere-like already at 700 °C (Figure S3-4.e). At 900 °C, for the nanorods with AR>4 the integrity of the silica shell is destructed and the gold cores were partially released or melted into larger spheres (Figure 4.c,d)

The lower stability of the higher AR nanorods was observed earlier by Zijlstra et al., who investigated laser-induced melting of bare gold nanorods with different aspect ratios [32]. They found that the higher the aspect ratio, the less stable is the nanorod and suggested that this is due to the larger surface energy of the higher AR nanorods. This explains the high shape-stability (up to 700 °C) of our smallest AR nanorods (Au1).

Based on the SEM images of the samples (Figure S1-3), the silica shell deforms together with the gold core for the Au1-Au3 nanorod samples. We reported this flexibility of the silica shell earlier [46]. The higher the aspect ratio of the gold core, the less intense is the shape transformation of the silica shell, as for Au4 nanorods the silica shell was not elastic enough to follow the shape change of the core after the 700 °C treatment (Figure S4.e, see example particles indicated with circles). At 900 °C, the silica shell broke up and released the gold

cores which in some cases melted into larger spheres, indicated with arrows on Figure 4.d. We attribute this finding to the high mechanical stress exerted on the shell by the deforming gold core for this type of nanorods. This assumption is also justified by the fact that this core has the highest volume, it seems that the required shape transformation is too large for the shell to follow it without any damage.

To investigate the role of the gold cores in the shape transformation of the shell, control experiments were performed with the silica shells of the Au2 and Au4 nanorods. After the core/shell particles were treated at 300 °C, the gold cores were dissolved using aqua regia (Figure 5.a,c). These empty shells were heated at 900 °C and in both cases, the silica shells preserved their rod-like shape with the same size (shell outer dimensions for Au2: 29x43 nm and for Au4: 32x54 nm, Figure 5.b,d). This means that the deformation of the silica shell observed for the core/shell particles is indeed induced by the shape change of the gold core due to the thermal treatment.

On the other hand the silica shell presented in this study improved the stability of the gold cores. It is important to stress that without silica coating the gold nanorods turn into nanospheres already at 250 °C [35]. The shape-protecting effect of the silica shell in optical heating experiments was investigated earlier and similar results to our findings were obtained [36]. In our case, upon heating in an oven for as long as one hour all particles with AR>3 remained rod-like up to 500 °C, whereas particles with AR<3 even up to 700 °C. This means that the silica coating can effectively protect the gold nanorod cores at higher temperatures depending on the aspect ratio.

4. Conclusion

Thermal treatment of solid-supported mesoporous silica-coated gold nanorods was investigated at different temperatures in the range of 300 °C and 900 °C. It was found that the silica shell effectively protected the nanorods from turning into nanospheres even up to 700 °C. For nanorods with AR=2.5 it was found that the silica shell protected the gold core from significant deformation up to 500 °C. In the case of nanorods with AR≥3 the aspect ratio after annealing monotonously decreased versus the temperature up to 900 °C. The stability of the nanorod cores decreased with increasing aspect ratio, as for AR>3 the nanorods became sphere-like already at 700 °C and the decrease of the AR with the increasing temperature was

more steep. The shape change of the nanorods is also reflected in the change of their optical properties as the aspect ratio decrease caused a blue shift in the longitudinal surface plasmon resonance peak. For nanorods with smaller aspect ratio the silica shell deformed together with the gold core. Contrarily, for the largest aspect ratio nanorod (AR=4.3) the shell could not follow the shape change of the gold cores even at 700 °C. At 900 °C the gold cores were partially released due to the break-up of the shell, resulting in larger spherical particles. It was confirmed that the temperature induced deformation of the silica shell during the heat treatment is initiated by the deformation of the embedded gold nanorod core.

Acknowledgment

This work was supported by the Hungarian Science Foundation (OTKA PD 105173), János Bolyai Research Fellowships from the Hungarian Academy of Sciences and EU FP7 “UNION” (Nr. 310250). We thank Blanka Mohácsi for the help with the nanorod preparation and Zsolt Zolnai for reading the manuscript.

REFERENCES

[1] Tsai, M.-F.; Chang, S.-H. G.; Cheng, F.-Y.; Shanmugam, V.; Cheng, Y.-S.; Su, C.-H.; Yeh, C.-S. Au Nanorod Design as Light-Absorber in the First and Second Biological Near-Infrared Windows for in Vivo Photothermal Therapy. *Acs Nano* **2013**, *7*, 5330-5342.

[2] von Maltzahn, G.; Park, J.-H.; Agrawal, A.; Bandaru, N. K.; Das, S. K.; Sailor, M. J.; Bhatia, S. N. Computationally Guided Photothermal Tumor Therapy Using Long-Circulating Gold Nanorod Antennas. *Cancer Research* **2009**, *69*, 3892-3900.

[3] Jokerst, J. V.; Thangaraj, M.; Kempen, P. J.; Sinclair, R.; Gambhir, S. S. Photoacoustic Imaging of Mesenchymal Stem Cells in Living Mice via Silica-Coated Gold Nanorods. *Acs Nano* **2012**, *6*, 5920-5930.

[4] Jokerst, J. V.; Cole, A. J.; Van de Sompel, D.; Gambhir, S. S. Gold Nanorods for Ovarian Cancer Detection with Photoacoustic Imaging and Resection Guidance via Raman Imaging in Living Mice. *Acs Nano* **2012**, *6*, 10366-10377.

[5] Choi, W. I.; Sahu, A.; Kim, Y. H.; Tae, G. Photothermal Cancer Therapy and Imaging Based on Gold Nanorods. *Annals of Biomedical Engineering* **2012**, *40*, 534-546.

[6] Huang, X. H.; El-Sayed, I. H.; Qian, W.; El-Sayed, M. A. Cancer cell imaging and photothermal therapy in the near-infrared region by using gold nanorods. *Journal of the American Chemical Society* **2006**, *128*, 2115-2120.

[7] Joy, N. A.; Janiszewski, B. K.; Novak, S.; Johnson, T. W.; Oh, S.-H.; Raghunathan, A.; Hartley, J.; Carpenter, M. A. Thermal Stability of Gold Nanorods for High-Temperature Plasmonic Sensing. *Journal of Physical Chemistry C* **2013**, *117*, 11718-11724.

[8] Chen, Y.-S.; Frey, W.; Walker, C.; Aglyamov, S.; Emelianov, S. Sensitivity enhanced nanothermal sensors for photoacoustic temperature mapping. *Journal of Biophotonics* **2013**, *6*, 534-542.

[9] Rosman, C.; Prasad, J.; Neiser, A.; Henkel, A.; Edgar, J.; Soennichsen, C. Multiplexed Plasmon Sensor for Rapid Label-Free Analyte Detection. *Nano Letters* **2013**, *13*, 3243-3247.

[10] Mayer, K. M.; Lee, S.; Liao, H.; Rostro, B. C.; Fuentes, A.; Scully, P. T.; Nehl, C. L.; Hafner, J. H. A label-free immunoassay based upon localized surface plasmon resonance of gold nanorods. *Acs Nano* **2008**, *2*, 687-692.

[11] Ullah, M. A.; Li, X.; Cheng, X.; Hao, X.; Su, Y.; Ma, J.; Gu, M. Low energy-density recording with a high-repetition-rate laser beam in gold-nanorod-embedded discs. *Optics Express* **2012**, *20*, 24516-24523.

[12] Chon, J. W. M.; Bullen, C.; Zijlstra, P.; Gu, M. Spectral encoding on gold nanorods doped in a silica sol-gel matrix and its application to high-density optical data storage. *Advanced Functional Materials* **2007**, *17*, 875-880.

[13] Nanda, K. K. Size-dependent melting of nanoparticles: Hundred years of thermodynamic model. *Pramana - J. Phys.* **2009**, *72*, 617-628.

[14] Gülseren, O.; Ercolessi, F.; Tosatti, E. Premelting of thin wires. *Phys. Rev. B* **1995**, *51*, 7377-7380.

[15] Allen, G. L.; Bayles, R.A.; Gile, W. W.; Jesser, W. A. Small particle melting of pure metals. *Thin Solid Films, 144* (1986) 297-308.

[16] Little, S.A.; Begou, T.; Collins, R. W.; Marsillac, S. Optical detection of melting point depression for silver nanoparticles via in situ real time spectroscopic ellipsometry. *Appl. Phys. Lett.* **2012**, *100*, 051107.

[17] Borel, J.-P. Thermodynamical size effect and the structure of metallic clusters. *Surf. Sci.* **1981**, *106*, 1-9.

[18] Goswami, G. K.; Nanda, K. K. Size-dependent melting of finite-length nanowires. *J. Phys. Chem. C* **2010**, *114*, 14327-14331.

[19] Jiang, Q.; Zhang, S.; Zhao, M. Size-dependent melting point of noble metals. *Mat. Chem. Phys.* **2003**, *82*, 225–227.

[20] Xue, Y.-Q.; Zhao, M.-Z.; Lai. W.-P. Size-dependent phase transition temperatures of dispersed systems. *Physica B* **2013**, *408*, 134-139.

[21] Lide, D. R. (Ed.); *CRC Handbook of Chemistry and Physics*, 89th ed., CRC Press Inc., Boca Raton, 2008.

[22] Setoura, K.; Werner, D.; Hashimoto, S. Optical scattering spectral thermometry and refractometry of a single gold nanoparticle under CW laser excitation. *J. Phys. Chem. C* **2012**, *116*, 15458-15466.

[23] Insawa, S.; Sugiyama, M.; Yamaguchi, Y. Laser-induced shape transformation of gold nanoparticles below the melting point: the effect of surface melting. *J. Phys. Chem. B* **2005**, *109*, 3104-3111.

[24] Plech, A.; Cerna, R.; Kotaidis, V.; Hudert, F.; Bartels, A.; Dekorsy, T. A surface phase transition of supported gold nanoparticles. *Nano Lett.* **2007**, *7*, 1026-1031.

[25] Canpean, V.; Gabudean, A. M.; Astilean, S. Enhanced thermal stability of gelatin coated gold nanorods in water solution. *Colloids and Surfaces a-Physicochemical and Engineering Aspects* **2013**, *433*, 9-13.

[26] Canevali, P.; Ercolessi, F.; Tosatti, E. Melting and nonmelting behavior of the Au(111) surface. *Phys. Rev. B* **1987**, *36*, 6701-6704.

[27] Hoss, A.; Nold, M.; Von Blanckenhagen, P.; Meyer, O. Roughening and melting of Au(110) surfaces. *Phys. Rev. B* **1992**, *45*, 8714-8720.

[28] Mochrie, S. G. J.; Zehner, D. M.; Ocko, B. M.; Gibbs, D. Structure and phases of the Au(001) surface: X-Ray scattering measurements. *Phys. Rev. Lett.* ***1990***, *64*, 2925-2928.

[29] Link, S.; Wang, Z. L.; El-Sayed, M. A. How does a gold nanorod melt? *Journal of Physical Chemistry B* **2000**, *104*, 7867-7870.

[30] Ma, H.; Bendix, P. M.; Oddershede, L. B. Large-Scale Orientation Dependent Heating from a Single Irradiated Gold Nanorod. *Nano Letters* **2012**, *12*, 3954-3960.

[31] Link, S.; El-Sayed, M. A. Spectroscopic determination of the melting energy of a gold nanorod. *Journal of Chemical Physics* **2001**, *114*, 2362-2368.

[32] Zijlstra, P.; Chon, J. W. M.; Gu, M. White light scattering spectroscopy and electron microscopy of laser induced melting in single gold nanorods. *Physical Chemistry Chemical Physics* **2009**, *11*, 5915-5921.

[33] Link, S.; Burda, C.; Nikoobakht, B.; El-Sayed, M. A. Laser-induced shape changes of colloidal gold nanorods using femtosecond and nanosecond laser pulses. *Journal of Physical Chemistry B* **2000**, *104*, 6152-6163.

[34] Hu, X.; Wang, T.; Dong, S. Thermal annealing of Au nanorod self-assembled nanostructured materials: Morphology and optical properties. *Journal of Colloid and Interface Science* **2007**, *316*, 947-953.

[35] Petrova, H.; Juste, J. P.; Pastoriza-Santos, I.; Hartland, G. V.; Liz-Marzan, L. M.; Mulvaney, P. On the temperature stability of gold nanorods: comparison between thermal and ultrafast laser-induced heating. *Physical Chemistry Chemical Physics* **2006**, *8*, 814-821.

[36] Chen, Y.-S.; Frey, W.; Kim, S.; Homan, K.; Kruizinga, P.; Sokolov, K.; Emelianov, S. Enhanced thermal stability of silica-coated gold nanorods for photoacoustic imaging and image-guided therapy. *Optics Express* **2010**, *18*, 8867-8877.

[37] Chen, Y.-S.; Frey, W.; Kim, S.; Kruizinga, P.; Homan, K.; Emelianov, S. Silica-Coated Gold Nanorods as Photoacoustic Signal Nanoamplifiers. *Nano Letters* **2011**, *11*, 348–354.

[38] Zhang, Z.; Wang, L.; Wang, J.; Jiang, X.; Li, X.; Hu, Z.; Ji, Y.; Wu, X.; Chen, C. Mesoporous Silica-Coated Gold Nanorods as a Light-Mediated Multifunctional Theranostic Platform for Cancer Treatment. *Advanced Materials* **2012**, *24*, 1418–1423.

[39] Takahashi, Y.; Miyahara, N.; Yamada, S. Gold Nanorods Embedded in Titanium Oxide Film for Sensing Applications. *Analytical Sciences* **2013**, *29*, 101-105.

[40] Khalavka, Y.; Ohm, C.; Sun, L.; Banhart, F.; Soennichsen, C. Enhanced thermal stability of gold and silver nanorods by thin surface layers. *Journal of Physical Chemistry C* **2007**, *111*, 12886-12889.

[41] Gautier, C.; Cunningham, A.; Si-Ahmed, L.; Robert, G.; Bürgi, T. Pigments based on silica-coated gold nanorods: Synthesis, colouring strength, functionalisation, extrusion, thermal stability and colour evolution. *Gold Bull.* **2010**, *43*, 94-104.

[42] Omura, N.; Uechi, I.; Yamada, S. Comparison of Plasmonic Sensing between Polymer- and Silica-Coated Gold Nanorods. *Analytical Sciences* **2009**, *25*, 255–259.

[43] Gorelikov, I.; Matsuura, N. Single-step coating of mesoporous silica on cetyltrimethyl ammonium bromide-capped nanoparticles. *Nano Letters* **2008**, *8*, 369-373.

[44] Pastoriza-Santos, I.; Pérez-Juste, J.; Liz-Marzán, L. M. Silica-Coating and Hydrophobation of CTAB-Stabilized Gold Nanorods. *Chem. Mater.* **2006**, *18*, 2465–2467.

[45] Jana, N. R.; Earhart, C.; Ying, J. Y. Synthesis of Water-Soluble and Functionalized Nanoparticles by Silica Coating. *Chem. Mater.* **2007**, *19*, 5074–5082.

[46] Gergely-Fülöp, E.; Nagy, N.; Deák, A. Reversible shape transition: Plasmonic nanorods in elastic nanocontainers. *Materials Chemistry and Physics* **2013**, *141*, 343-347.

[47] Ye, X.; Jin, L.; Caglayan, H.; Chen, J.; Xing, G.; Zheng, C.; Vicky, D.-N.; Kang, Y.; Engheta, N.; Kagan, C. R.; Murray, C. B. Improved Size-Tunable Synthesis of Monodisperse Gold Nanorods through the Use of Aromatic Additives. *Acs Nano* **2012**, *6*, 2804-2817.

[48] Fülöp, E.; Nagy, N.; Deák, A.; Bársony, I. Langmuir-Blodgett films of gold/silica core/shell nanorods. *Thin Solid Films* **2012**, *520*, 7002-7005.

[49] Link, S.; Mohamed, M. B.; El-Sayed, M. A. Simulation of the optical absorption spectra of gold nanorods as a function of their aspect ratio and the effect of the medium dielectric constant. *Journal of Physical Chemistry B* **1999**, *103*, 3073-3077.

Figure captions

Table 1 Aspect ratios, sizes and longitudinal or main peak positions of the starting and the heat-treated silica-coated gold nanorods. The longitudinal peak position of the starting Au4 nanorods is not presented here as it was outside of the detection range of our spectrometer. For Au1 and Au2 treated at 900 °C, Au3 and Au4 over 700 °C only one extinction peak can be observed due to the nearly isotropic shape of the particles.

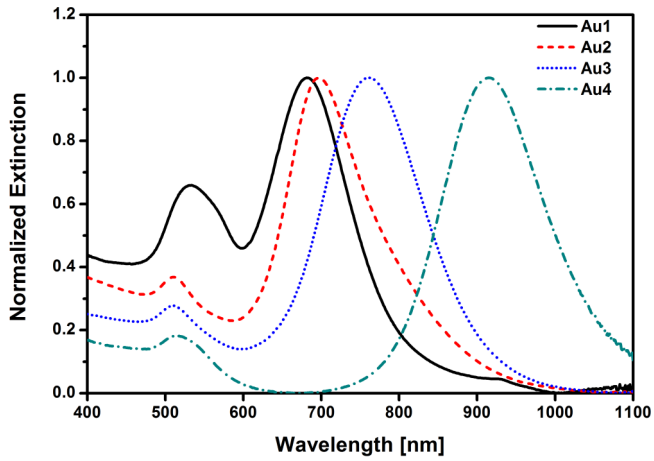

Figure 1 Normalized extinction spectra of the as-prepared nanorods Au1-Au4. The longitudinal peak position red shifts with increasing aspect ratio.

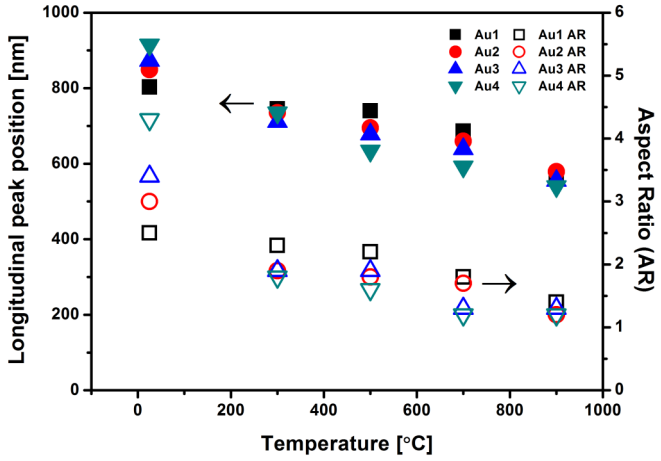

Figure 2 Longitudinal extinction peak positions (left axis, solid symbols) and aspect ratios (right axis, open symbols) of the silica-coated gold nanorods after thermal treatment.

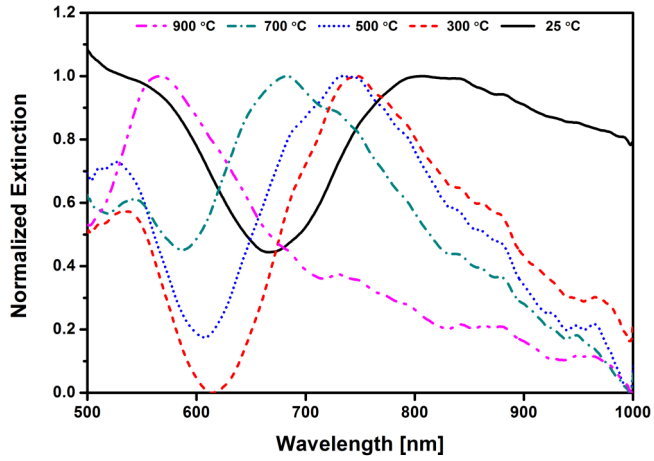

Figure 3 Normalized extinction spectra of the Au1 nanoparticles at room temperature and after annealing at different temperatures.

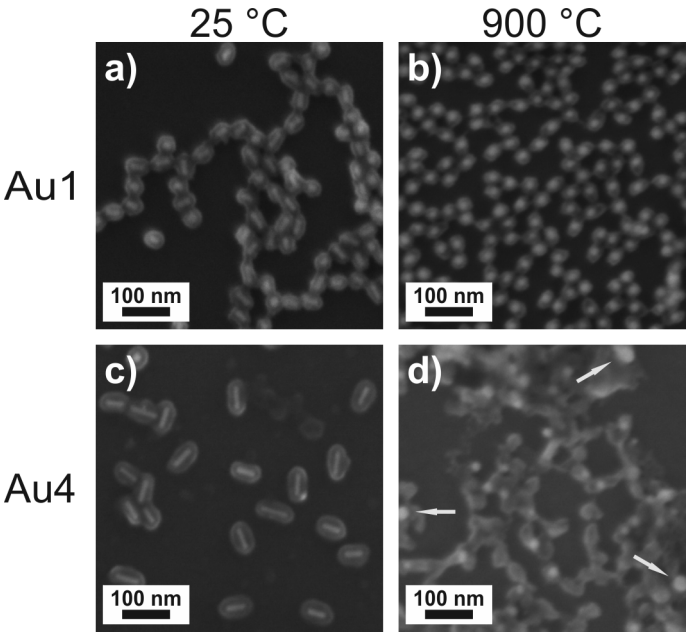

Figure 4 SEM images of the Au1 nanoparticles at a) room temperature and b) after the heat treatment at 900°C. (c-d) The same for Au4 nanoparticles. In image d) the arrows mark large spherical gold particles coalesced from the released gold cores after the break-up of the shell.

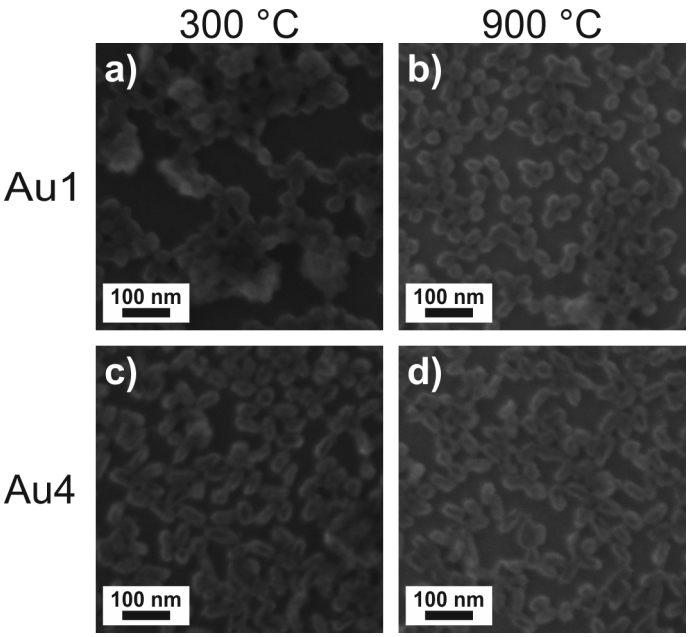

Figure 5 Silica shells of the a) Au1 and c) Au4 nanorods after annealing the core/shell structures at 300 °C and dissolving the cores with aqua regia. After annealing at 900 °C the shells remain rod-like as can be seen in b) for Au1 and d) for Au4, respectively.